Enrichment of potent GSK-3β inhibitors from docking studies in the enzyme active site

Pravin Kumar Gadakar, Samiron Phukan, Prasanna M. Dattatreya and V. N. Balaji*

Structure Directed Molecular Design Group, Jubilant Biosys Limited, #96, Industrial Suburb, 2nd Stage, Yeshwanthpur, Bangalore 560 022, India

We have presented molecular docking studies using Glide, in the active sites of the X-ray crystal structures and induced fit models of glycogen synthase kinase-3β (GSK-3β). Using the docking score as the ranking metric, we have computed the enrichment of known GSK-3β inhibitors which are seeded in a decoy set of World Drug Index compounds. Interestingly, our studies have found that extra precision docking of compounds into the ensemble of protein structures either from X-ray data or induced fit models and ranking them by GlideScore, lead to the best retrieval of actives in the top 5% and 10% of the database with significant enrichment. Our studies emphasize the significance of induced fit models in such enrichment when experimental data are limited.

Keywords: Database, enrichment, glycogen synthase kinase-3β, induced fit docking, molecular docking studies.

GLYCOGEN synthase kinase-3β (GSK-3β) is a unique multifunctional serine/threonine kinase that is inactivated by phosphorylation. In response to insulin binding, PKB/AKT phosphorylates GSK-3β on serine 9, which prevents the enzyme from phosphorylating glycogen synthase[1–3]. Unphosphorylated glycogen synthase is active and able to synthesize glycogen. Thus it plays a key role in the transduction of regulatory and proliferative signals arising out at the cell membrane in the insulin signalling pathway, leading to potential modulation of blood glucose levels[4]. GSK-3β inhibitors have been discovered and developed as potential therapeutics against type-2 diabetes[5]. GSK-3β is also unique in that it requires a substrate that has been phosphorylated by a distinct kinase before it can phosphorylate the substrate.

In addition to insulin signaling, GSK-3β participates in the Wingless Integration (*WNT*) gene signaling pathway, where it forms a complex with axin, β-catenin and adenomatous polyposis coli protein[6]. In the presence of WNTs, GSK-3β is unable to phosphorylate β-catenin, which leads to stabilization of β-catenin. GSK-3β has been linked to a diverse array of diseases like muscle hypertrophy, cancer, bipolar mood disorder, schizophrenia and diabetes. In addition, there is considerable interest in the clinical role of GSK-3β inhibitors because they may mimic the effect of insulin or reduce the hyper-phosphorylation of Tau protein observed in Alzheimer's disease[7]. Phosphorylation of Tau by GSK-3β modulates its ability to organize microtubules into ordered arrays such as those found in axons[1].

Considerable interest has been devoted to the elucidation of the structure of GSK-3β and the interactions with its inhibitors and substrate analogues. To date, thirteen high to moderately resolved (resolution of 1.95 to 2.8 Å) X-ray structures (1GNG, 1H8F, 1I09, 1J1B, 1J1C, 1O9U, 1PYX, 1Q3D, 1Q3W, 1Q41, 1Q4L, 1Q5K and 1UV5)[8–16] are documented in the Protein Data Bank (PDB)[17]. In addition, one X-ray complex is recorded in patent literature[18]. An overlap of some of these structures shown in Figure 1, clearly demonstrates two distinct ligand-binding sites. One of them corresponds to the so-called active site and the other to the phosphorylation site. A number of different chemical classes of compounds (Figure 2) bind to these two sites and their interactions with the active site residues are stabilized by hydrogen-bonding networks. In most of the X-ray structures, these inter-

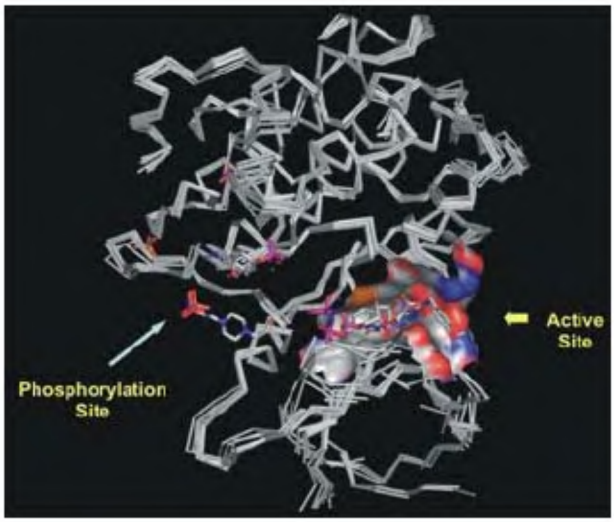

Figure 1. Overlap of X-ray structures of GSK-3β (1H8F, 1O9U, 1PYX, 1Q4L, 1Q5K and 1UV5). The ligand in 1H8F (4-(2-hydroxyethyl)-1-piperazine ethanesulfonic acid) is bound in the phosphorylation site.

*For correspondence. (e-mail: vnbalaji@jubilantbiosys.com)

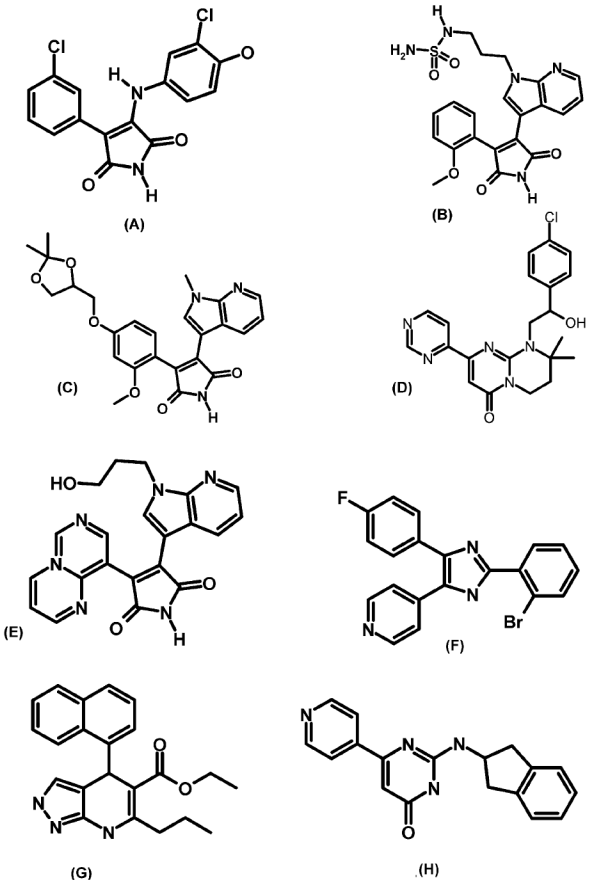

Figure 2. Schematic illustration of representative chemotypes found in the set of 10 GSK-3β actives used in enrichment studies.

actions are mediated by at least one molecule of water. Recently, in addition to structural elucidation, 3D-QSAR studies using CoMFA have been presented on a specific class of GSK-3β inhibitors. The results of the CoMFA analyses did not correspond to the active-site interactions, but claim to characterize the fundamental features of the receptor–ligand interactions[19].

In light of the biological significance of GSK-3β in various disease areas and in light of the availability of high-resolution X-ray structure data, we have undertaken molecular modelling studies to determine optimal protocols useful for discovering potential inhibitors with novel templates. Toward this goal, we have carried out docking studies in the active site of GSK-3β using Schrödinger docking and simulation tools on six of the X-ray structures and on protein models induced to fit non-cognate ligands. Specifically, we have focused our attention in this study on the enrichment of known actives seeded in a collection of decoys. Our studies clearly demonstrate that the more accurate extra precision (XP) docking leads to greater enrichment of the actives seeded amongst decoys than that obtained by (standard precision (SP) docking. We also demonstrate that in the event of limited availability of X-ray data, an ensemble of available structure data and induced fit models can be employed to enhance recovery of actives from a database of compounds. Thus, the XP-docking based protocol is established to be important in the identification of actives that tend to bind to the active site with the right profile of interactions. Furthermore, our studies provide valuable insights into the role of key active-site residues in the interactions of potential inhibitors with the enzyme active-site.

Methods and nomenclature

Ligand preparation

The three-dimensional structures of ten known GSK-3β inhibitors (Figure 2) and 1990 decoy molecules (chosen randomly as a subset of 20,000 World Drug Index (WDI) compounds) were prepared using the LigPrep module of Maestro v7.0.113 in the Schrödinger suite of tools[19]. The bond orders of these ligands were fixed and the ligands 'cleaned' through LigPrep specifying a pH value of 7.0. Most probable tautomers of the compounds were chosen based on their interactions with the protein in the X-ray structures. In the final stage of LigPrep, the compounds were energy minimized with Merck Molecular Force Field (MMFF)[20].

The active inhibitors belong to eight distinct chemotypes and span a molecular weight range of 300 to 500. The decoy set of molecules also span the same range of molecular weight and have at least 200 different chemotypes represented in it. Figure 3 *a–d* shows the histograms of distribution of molecular weight, log *P* and number of hydrogen-bond donors and acceptors for both the active and decoy sets. It may be observed that the property distribution of decoys are similar to that of actives, except in log *P* distribution, wherein actives have log *P* concentrated in the region of 2–4 (Figure 4 *b*). In other words, the property distribution also indicates that there is enough diversity in the decoys as well as actives considered in the study.

Protein preparation

Six out of seven PDB structures (available at the time of study) were chosen for the investigations, excluding the *apo*-structure, 1GNG. The PDB coordinates of the X-ray complexes (1H8F, 1O9U, 1PYX, 1Q5K and 1UV5) were aligned to the crystal structure 1Q4L (selected randomly), using the protein alignment tools in Maestro. This allows for the superposition of all the protein chains and ligands in a common framework of the protein active site and the phosphorylation site. All the crystallographic water molecules were deleted with the exception of those forming

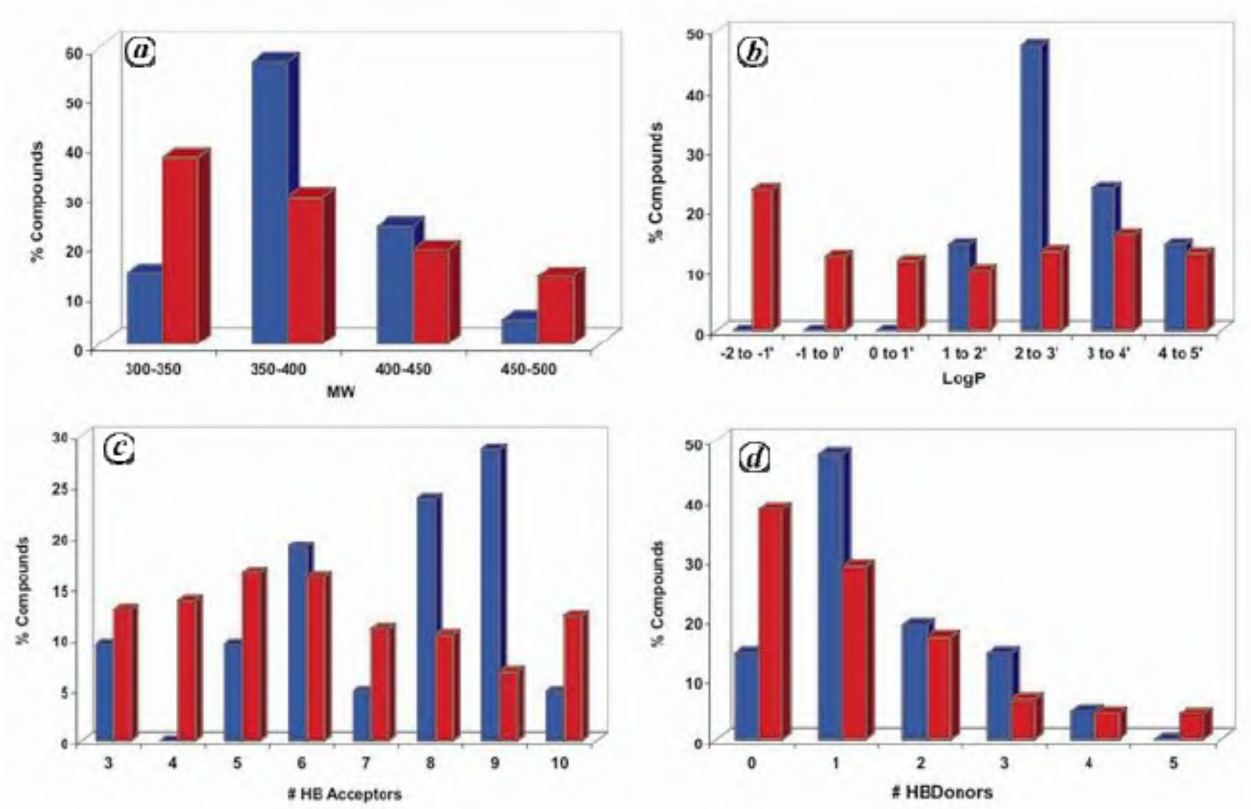

Figure 3. Distribution of molecular weight (MW) (***a***), log *P* (***b***), H-bond acceptors (***c***), and H-bond donors (***d***) values in the set of actives (■) and decoy molecules (■) used in the enrichment studies.

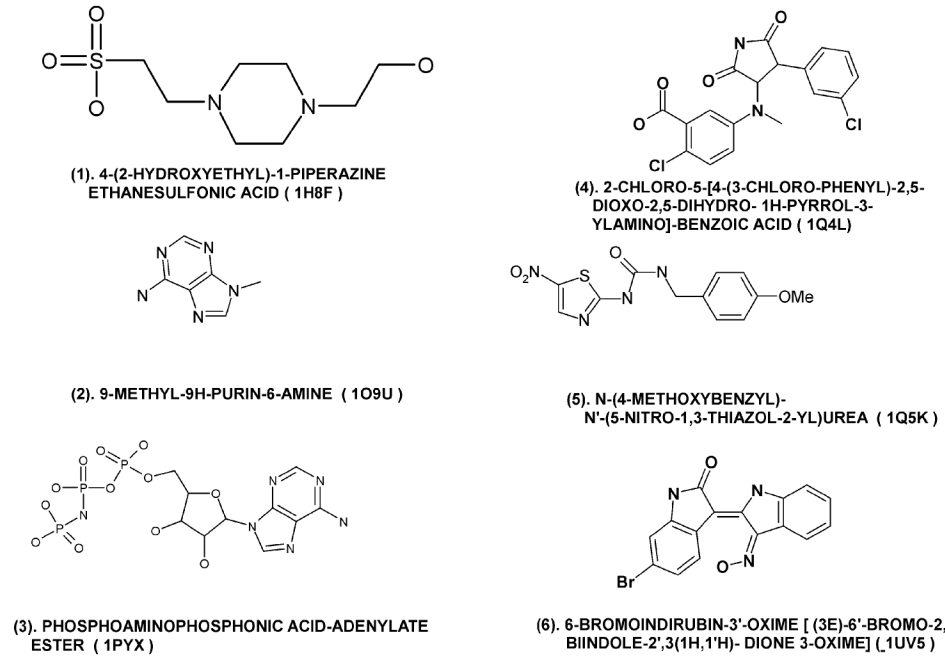

Figure 4. Schematic illustration of ligands in (**1**) 1H8F, (**2**) 1O9U, (**3**) 1PYX, (**4**) 1Q4L, (**5**) 1Q5K and (**6**) 1UV5.

bridge interactions between the protein residues and ligand atoms. In the case of 1PYX, two active-site magnesium ions were also retained as part of the protein. Once aligned, hydrogens were added to all the protein–ligand complexes, which were initially subjected to single-point energy calculation using the protein modelling package, Prime. This calculation was carried out using OPLS-2001 force field incorporating implicit solvation[21]. This process allows for the addition of missing side-chain atoms to the protein residues. The guanidines and ammonium groups in all the arginine and lysine side chains were made cationic and the carboxylates of aspartate and glutamate residues were made anionic. Asn185 side-chain amides were flipped by 180° to optimize the interactions with the X-ray ligands. In addition, the Asp200 side-chain carboxylate was treated in a neutral form in the protein structures of all the complexes, with the exception of 1PYX. This is necessary in light of the fact that the binding of the ligand in 1PYX is stabilized by two magnesium ions bound to Asp200 carboxylate. However, there are no Mg^{2+} ions present in any of the other five crystal structures.

Following the above steps of preparation, the protein–ligand complexes in the X-ray structures were subjected to energy minimization using the Schrödinger implementation of OPLS-2001 force field with implicit solvation[22] in two stages. In the first stage, the positions of water molecule/s and/or active-site Mg^{2+} ions were optimized keeping the ligand and the protein atoms in their X-ray structure positions. In the second stage, the entire complex was minimized and minimization terminated when the root mean square deviation (RMSD) of the heavy atoms in the minimized structure relative to the X-ray structure exceeded 0.3 Å. This helps maintain the integrity of the prepared structures relative to the corresponding experimental structures, while eliminating severe bad contacts between heavy atoms.

Docking studies

Docking studies on LigPrep-treated actives and decoys were carried out in the active sites of 1H8F, 1O9U, 1PYX, 1Q4L, 1Q5K and 1UV5 using the Schrödinger docking program[23,24], Glide. The protein–ligand complexes prepared as described above were employed to build energy grids using the default value of protein atom scaling (1.0) within a cubic box of dimensions 34 Å × 34 Å × 34 Å centred around the centroid of the X-ray ligand pose. The bounding box (within which the centroid of a docked pose is confined) dimensions were set to 14 Å × 14 Å × 14 Å. The best docked pose (with lowest GlideScore value) was saved per ligand. The representative results of XP docking scores are provided in Table 1. In the case of 1H8F, GlideScore was not good and this was improved subsequently in induced fit docking.

Induced fit docking studies

We have carried out induced fit docking studies on the 1Q5K protein model, wherein induced fit models have been obtained to fit ligands in non-cognate structures. In other words, the 1Q5K protein structure was induced to fit the ligands of 1Q4L, 1PYX, 1O9U and 1UV5. We have used the procedure described by Sherman *et al.*[25] via a Python script executed in the framework of Maestro v7.0.113. For the protein model, initial docking was performed with a grid (defined using centroid of the ligand) with default parameters. Twenty poses were chosen to be saved after initial Glide docking, which was carried out with van der Waals scaling of 0.4 for both protein and ligand non-polar atoms. After obtaining initial docked poses, Prime side chain and backbone refinement together with the minimization of the docked pose were carried out within a sphere of 5 Å from each pose saved. Glide re-docking was carried out in Prime refined structures having Prime energy values within 20 kcal/mol of the lowest energy value. The RMSD values of the ligand poses having best induced fit docking (IFD) score relative to the corresponding X-ray poses were determined. Higher ranked poses (2–5) of the induced fit docking score were also considered for RMSD calculations.

Enrichment studies

In order to identify GSK-3β protein models suitable for enrichment of active inhibitors of the enzyme, SP and XP docking studies were carried out on the 'database' of 2000 ligands (10 actives seeded amongst 1990 decoy molecules) in the active sites of 1H8F, 1O9U, 1PYX, 1Q4L, 1Q5K and 1UV5. This database has a random hit rate of 0.5% (=10*100/2000). As stated earlier, the top-ranked pose for each docked ligand (based on GlideScore) was saved. Percentages of actives retrieved in the top 5% (100) and 10% (200) of the database ranks were counted. In addition to looking at the retrieval of actives in individual structures, we have also considered such retrieval from the ensemble of protein structures. Toward this end, all the hits obtained by docking into each of the members of the ensemble were pooled and re-ranked using

Table 1. Representative XP docking results of cognate docking of complexed ligands to active site of corresponding GSK-3β X-ray structures

PDB ID	XP GlideScore	XP Glide energy (kcal/mol)
1H8F	–5.27	–33.60
1O9U	–8.71	–24.67
1PYX	–11.55	–71.25
1Q4L	–13.38	–57.19
1Q5K	–9.25	–46.23
1UV5	–16.13	–54.38

GlideScore. Redundancy in the hits obtained was eliminated; for each hit, only the model/pose with the lowest GlideScore was retained. This was followed by the counting of actives retrieved from the top 100 (5%) and 200 (10%) ranks.

Results and discussion

Validation of docking X-ray ligands

Before carrying out docking studies with the database ligands, the default docking protocol (including a van der Waals scaling of 0.8 for ligand atoms) was validated with the poses obtained for X-ray ligands in cognate (self) docking studies. Thus, for example, ligands (**4**) and (**5**) (Figure 4) were docked in the active sites of 1Q4L and 1Q5K respectively. The validation process consisted of two parts: (i) retention of key interactions seen in the native X-ray complex and (ii) RMSD values of less than 2 Å between the heavy atoms of the top-ranked docked pose and the X-ray pose. Cognate docking in all the active sites yielded top-ranked poses within 2 Å of the corresponding X-ray poses (details published elsewhere). Some of the key interactions observed in X-ray complexes and conserved in docked poses are described in the following paragraphs.

Ligand (**1**) in 1H8F is bound in the phosphorylation site with ionic interactions between the SO_3^{2-} moiety on the ligand and the side chains of Arg96, Arg180 and Lys205 on the protein. In addition, the SO_3^{2-} moiety forms stabilizing electrostatic interactions with phenolic hydroxyl group in the aromatic side chain of Tyr216.

In the case of ligands bound in the active site of the GSK-3β crystal structures (**2**–**6**), four out of five form hydrogen bond interactions with the backbone carbonyl oxygen of Asp133 (Figure 5*a*–*f*). The only exception to this bonding is the ligand in 1Q5K (**5**), which forms hydrogens bonds both the N-H and C=O moieties of Val135 (Figure 5 *e*). However, all the five ligands form hydrogen bonds with the backbone N-H or C=O of Val135. In addition, these ligands are also hydrogen bonded to active-site waters, which hydrogen bond with the backbone NH moiety of Asp200 or the side-chain amide of Gln186. Furthermore, the aromatic phenol in Tyr134 provides hydrophobic stabilization to most of the ligands (**3**–**6**) in the active site (Figure 5 *c*–*f*). All these interactions are conserved in corresponding top-ranked docked poses (details published elsewhere).

Enrichment studies

We have utilized the protein structures from the X-ray crystal data (1H8F, 1O9U, 1Q4L, 1Q5K, 1UV5 and 1PYX) and protein models obtained by induced fit docking of non-cognate ligands to carry out enrichment studies. Since the results obtained for docking in the 'active site' of 1H8F protein model are identical to those obtained with 1Q5K, data for the former are not discussed further. Also, the induced fit models employed in the enrichment docking studies are obtained by inducing the protein structure in 1Q5K to bind to ligands (**2**), (**4**) and (**6**) (details published elsewhere). These studies help us identify the optimal protocol for the highest enrichment of actives in the top 5 and 10% of the database GlideScore ranks.

Table 2 shows the retrieval of GSK-3β actives seeded into the decoy database as described earlier, from SP and XP docking into the X-ray structures of 1O9U, 1PYX, 1Q4L, 1Q5K and 1UV5. Specifically, percentages of active compounds recovered in the top 5 and 10% of the GlideScore ranks are listed. The results of ensemble docking into these five crystal structures are also illustrated in Table 2 (last row).

The results indicate that at least half the actives are retrieved in the top 5% (100) of the SP docking ranks in two out of the five X-ray structures, while three out of five structures do so in the top 5% of XP docking ranks. As is to be expected, larger percentages of actives are retrieved in the top 10% (200) of the database ranks in all the X-ray structures. Of particular interest are the cases of docking the database of actives and decoys into the active sites of 1Q5K and 1PYX proteins. In the case of 1Q5K, no actives are retrieved in the top 5% of either SP or XP docking, while only one out ten actives is retrieved in the top 10%. No actives are retrieved by SP docking into the 1PYX active site within 10% of the ranks, while 40% of the actives are obtained in the top 100 and 200 ranks in XP docking. Ensemble docking into the five proteins retrieves at least 70% of the actives within the top 5% of the GlideScore ranks, while the corresponding percentage is 90 when the top 10% of the ranks is considered. Thus, it is clear that upon SP docking of the database, screening the top 10% of the ranks will recover 90% of the actives yielding a nine-fold enrichment of actives. In the case of XP docking into the five-protein ensemble, an 18-fold enrichment is obtained since 90% of the compounds are recovered in the top 5% of the GlideScore ranks (Table 3). It can be noted that the enrichment in XP docking results are better than those of SP docking. This can be attributed to incorporation of additional terms in XP

Table 2. Percentage of actives recovered by the top 5 and 10% of the database ranked by GlideScores obtained in SP and XP docking protocols in the active sites of GSK-3β X-ray structures. Also shown are the retrieval percentages obtained in the ensemble of protein structures

Protein ↓	SP (5%)	SP (10%)	XP (5%)	XP (10%)
1O9U	40	60	60	80
1PYX	0	0	40	40
1Q4L	80	80	90	90
1Q5K	0	10	0	10
1UV5	50	60	60	60
Ensemble	70	90	90	90

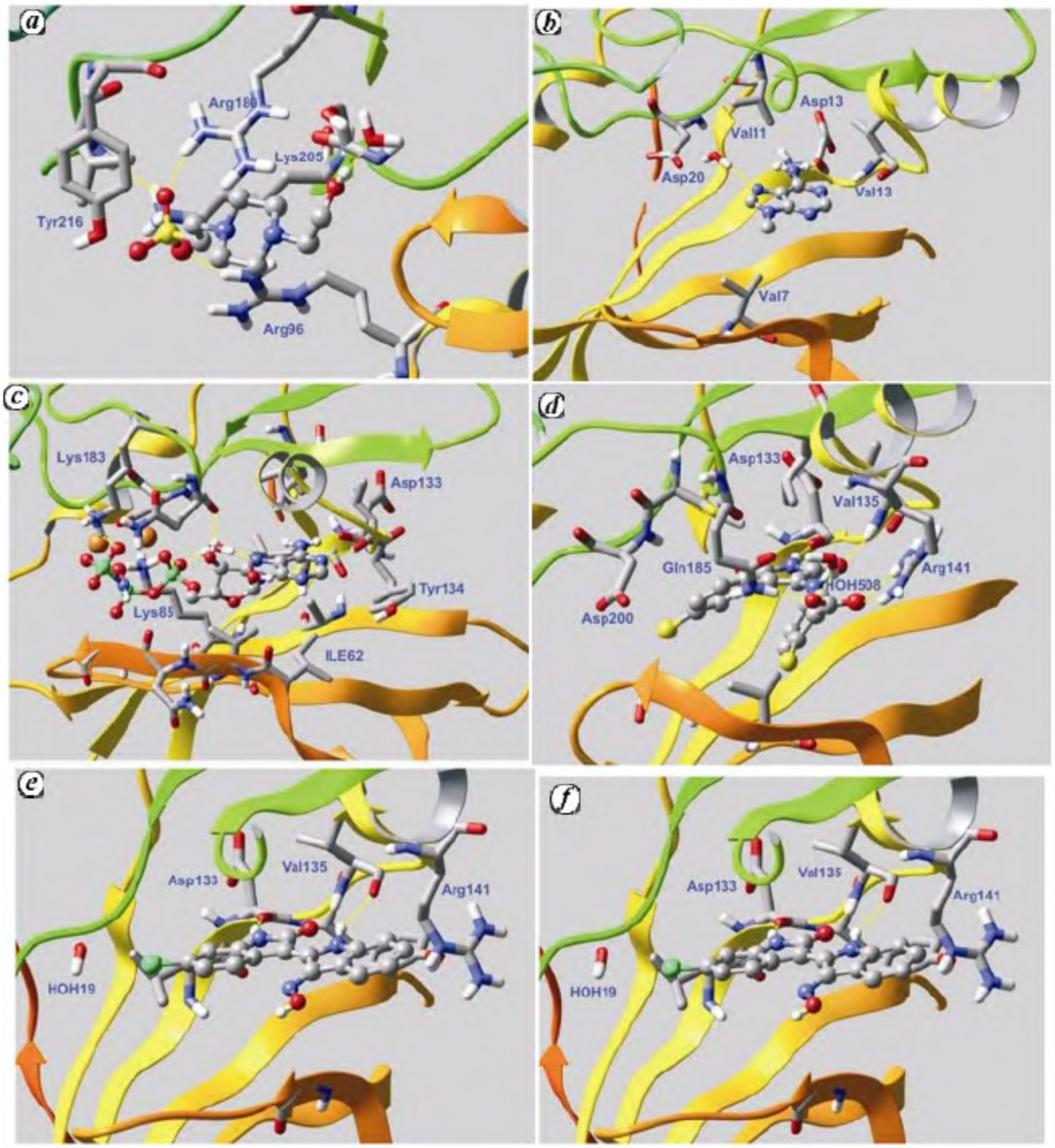

Figure 5. ***a***, Illustration of ligand binding site in 1H8F. Ligand (**1**) is docked in the phosphorylation site with ionic interactions between the SO_3^{2-} moiety on the ligand and the side chains of Arg96, Arg180 and Lys205 on the protein. The side chain of Tyr216 is also shown for perspective. ***b***, Illustration of ligand binding site in 1O9U. Ligand (**2**) is docked in the active site with hydrogen bonding interaction with the backbone carbonyl of Asp133 and N-H of Val135. Also shown is the active site water HOH56, which hydrogen bonds to one of the five-membered ring nitrogens. ***c***, Illustration of ligand binding site in 1PYX. Ligand (**3**) is docked in the active site with ionic interactions between the phosphate moieties on the ligand and the side chains of Lys85 and Lys183 on the protein. The ligand pose in the X-ray structure is also stabilized by two magnesium ions in the active site (orange spheres). ***d***, Illustration of ligand binding site in 1Q4L. Ligand (**4**) is docked in the active site with a network of hydrogen-bonding interactions with Asp133, Val135, Gln185 and Arg141. Also shown is HOH508, which interacts with the acid group on one of the phenyl rings in the ligand and with Gln185 side chain carbonyl oxygen. ***e***, Illustration of ligand binding site in 1Q5K. In this protein–ligand complex, ligand (**5**) does not form hydrogen bonds with the Asp133 carbonyl as observed in 1Q4L, 1O9U, 1PYX and 1UV5. ***f***, Illustration of ligand binding site in 1UV5. Ligand (**6**) is docked in the active site with hydrogen-bonding interaction with the backbone C=O of Asp133 and N-H of Val135. The active site water molecule HOH19 trapped between the ligand and nearby protein residue does not form any hydrogen-bonding interactions with the ligand atoms.

Table 3. Percentage of actives recovered by the top 5 and 10% of the database ranked by GlideScores obtained in SP and XP docking protocols in the active sites of GSK-3β X-ray structure 1Q5K and its models induced to fit ligands (**2**) (IF_1O9U), (**4**) (IF_1Q4L) and (**6**) (IF_1UV5). Also shown are the retrieval percentages obtained in the ensemble of protein structures from X-ray structure and induced fit models

Protein ↓	Top 5% (SP)	Top 10% (SP)	Top 5% (XP)	Top 10% (XP)
1Q5K (X-ray)	0	10	0	10
IF_1O9U	10	10	60	70
IF_1Q4L	30	50	80	90
IF_1UV5	10	20	30	40
Ensemble	30	50	50	50

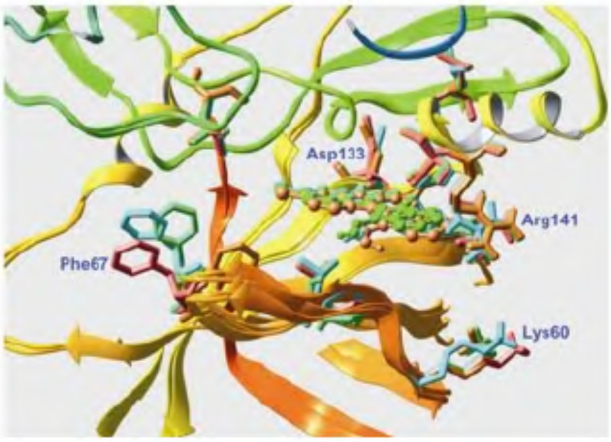

Figure 6. An overlay of ligand (**6**) in X-ray pose (cyan) and top two IFD score-ranked poses in the induced fit model 1Q5K_1UV5 (green and brown). Also shown is the X-ray crystal structure of 1Q5K aligned to the three models (pink). The position of side chain of Phe67 in the top-ranked induced model (brown) has been significantly deviated from the side chain in the second ranked induced fit model and the X-ray structures of 1UV5 (cyan) and 1Q5K (pink).

scoring function, and this observation is consistent with that of an earlier report[25].

In addition to crystal structures, we have also examined the enrichment of actives by SP and XP docking in the active site of induced fit models. As an example, we have chosen the models of 1Q5K induced to fit ligands (**2**), (**4**) and (**6**). The results of these docking studies are outlined in Table 3.

As stated earlier, only one out of ten actives is retrieved by either SP or XP docking in the active site of 1Q5K crystal structure (row 1, Table 3; row 5, Table 2). However, there is significant improvement in the retrieval of actives by the three induced fit models (Table 3), with the exception of SP docking into the active site of 1Q5K_1O9U. Here only one compound is returned in the top 5 and 10% of the ranks. Interestingly, retrieval of actives by SP docking in an ensemble of 1Q5K crystal structure and three induced fit models is better than that of the crystal structure and two of the induced fit models (1Q5K_1O9U, 1Q5K_1UV5). However, it is the same as that obtained in 1Q5K_1Q4L. On the other hand, XP docking in the ensemble retrieves fewer actives than by the induced fit models, 1Q5K_1O9U and 1Q5K_1Q4L. However, these retrieval percentages are higher than those obtained from docking to the binding pockets of the X-ray structure and that of the induced fit model, IF_1UV5.

It is worth noting that the IF_1UV5 model was unable to retrieve as many actives as the other induced fit models. To investigate this, we analysed the side-chain conformations of active site residues. It was observed that variations in the side chains are mostly limited to the lower side of the ligand pose (relative to the region Asp133–Val135, Figure 6). The conformation Phe-67 on the loop between two β-strands, swings into the active site relative to X-ray conformation in the first top-ranked IFD model and in the second top-ranked IFD model the orientation is conserved (Figure 6). However, these conformational changes will not explain the observed anomaly in the retrieval of actives. Inclusion of explicit waters in the modelling might provide better clues towards an explanation.

The above results clearly demonstrate the utility of induced fit models in the enrichment actives, particularly when limited X-ray data are available. Thus, the lack of retrieval of most actives in the top 10% of the database ranks by XP or SP docking in the active site is compensated by corresponding docking in the active sites of induced fit models, which enrich considerably a larger number of actives. The ensemble docking is also helpful, although not to the same extent as in the case of the ensemble of X-ray structures.

Conclusion

We have presented enrichment studies in the active sites of six GSK-3β kinase X-ray structures. The induced fit models are clearly useful in the enhanced recovery of actives in enrichment studies carried out with SP and XP docking methods. Generally, higher enrichment is obtained by XP docking compared to SP docking. Larger enrichments are obtained by docking into an ensemble of X-ray structures versus the corresponding docking into an ensemble of an X-ray structure and its induced fit models.

1. Frame, S., Cohen, P. and Biondi, R. M., A common phosphate binding site explains the unique substrate specificity of GSK3 and its inactivation by phosphorylation. *Mol. Cell*, 2001, **7**, 1321–1327.
2. Mukai, F., Ishiguro, K., Sano, Y. and Fujita, S. C., Alternative splicing isoform of tau protein kinase I/glycogen synthase kinase 3β. *J. Neurochem.*, 2002, **81**, 1073–1083.
3. Doble, B. W. and Woodgett, J. R., GSK-3: Tricks of the trade for a multi-tasking kinase. *J. Cell Sci.*, 2003, **116**, 1175–1186.

4. McManus, E. J., Sakamoto, K., Armit, L. J., Ronaldson, L., Shapiro, N., Marquez, R. and Alessi, D. R., Role that phosphorylation of GSK3 plays in insulin and Wnt signalling defined by knockin analysis. *EMBO J.*, 2005, **24**, 1571–1583.
5. Wagman, A. S., Johnson, K. W. and Bussiere, D. E., Discovery and development of GSK3 inhibitors for the treatment of type 2 diabetes. *Curr. Pharm. Des.*, 2004, **10**, 1105–1137.
6. Li, L. *et al.*, Axin and Frat1 interact with Dvl and GSK, bridging Dvl to GSK in Wnt-mediated regulation of LEF-1. *EMBO J.*, 1999, **18**, 4233–4240.
7. Bhat, R. V. and Budd, S. L., GSK3β signalling: Casting a wide net in Alzheimer's disease. *Neurosignals*, 2002, **11**, 251–261.
8. Bax B. *et al.*, The structure of phosphorylated GSK-3β Complexed with a Peptide, FRATtide, that inhibits β-catenin Phosphorylation. *Structure*, 2001, **9**, 1143–1152.
9. Dajani, R., Fraser, E., Roe, S. M., Young, N., Good, V., Dale, T. C. and Pearl, L. H., Crystal structure of glycogen synthase kinase 3β: Structural basis for phosphate-primed substrate specificity and autoinhibition. *Cell*, 2001, **105**, 721–732.
10. Ter Haar, E., Coll J. T., Austen D. A., Hsiao, H. M., Swenson, L. and Jain, J., Structure of GSK3β reveals a primed phosphorylation mechanism. *Nature Struct. Biol.*, 2001, **8**, 593–596.
11. Dajani, R., Fraser, E., Roe, S. M., Yeo, M. and Good. V. M. and Thompson. V., Structural basis for recruitment of glycogen synthase kinase 3β to the axin-APC scaffold complex. *EMBO J.*, 2003, **22**, 494–501.
12. Bertrand, J. A. *et al.*, Structural characterization of the Gsk-3β active site using selective and non-selective ATP-mimetic inhibitors. *J. Mol. Biol.*, 2003, **333**, 393–407.
13. Bhat, R. *et al.*, Structural insights and biological effects of glycogen synthase kinase 3-specific inhibitor Ar-A014418. *J. Biol. Chem.*, 2003, **278**, 45937–45945.
14. Meijer, L. *et al.*, Gsk-3-selective inhibitors derived from Tyrian purple indurubins. *Chem. Biol.*, 2003, **10**, 1255.
15. Bussiere, D. E., He M., Le, V. P., Jansen J. M., Chin, S. M. and Martin, E., Crystallization and crystal structure of human glycogen synthase kinase 3β protein and methods of use thereof. Chiron Corporation, USA, International Application No. WO 0224893, 2002.
16. Aoki, M. *et al.*, Structural insight into nucleotide recognition in tau-protein kinase I/glycogen synthase kinase 3 beta. *Acta Crystallogr. Sect. D*, 2004, **60**, 439–446.
17. Berman, H. M. *et al.*, The protein data bank. *Nucleic Acids Res.*, 2000, **28**, 235–242.
18. Lescot, E., Bureau, R., de Oliveira Santos, J. S., Rochais, C., Lisowski, V., Lancelot, J. C. and Rault, S., 3D-QSAR and docking studies of selective GSK-3β inhibitors. comparison with a thieno[2,3-b]pyrrolizinone derivative, a new potential lead for GSK-3β ligands. *J. Chem. Inf. Model.*, 2005, **45**, 708–715.
19. Maestro (v7.0.113) – A unified interface for all Schrodinger products, developed and marketed by Schrodinger, LLC. NY, Copyright 2005; http://www.schrodinger.com
20. Halgren, T. A., Merck molecular force field. I. Basis, form, scope, parameterization and performance of MMFF94. *J. Comput. Chem.*, 1996, **17**, 490–519; Halgren, T. A., Merck molecular force field. II. MMFF94 van der Waals and electrostatic parameters for intermolecular interactions. *J. Comput. Chem.*, 1996, **17**, 520–552; Halgren, T. A., Merck molecular force field. III. Molecular geometrics and vibrational frequencies for MMFF94. *J. Comput. Chem.*, 1996, **17**, 553–586; Halgren, T. A. and Nachbar, R. B., Merck molecular force field. IV. Conformational energies and geometries. *J. Comput. Chem.*, 1996, **17**, 587–615; Halgren, T. A., Merck molecular force field. V. Extension of MMFF94 using experimental data, additional computational data and empirical rules. *J. Comput. Chem.*, 1996, **17**, 616–641; Halgren, T. A., MMFF VI. MMFF94s option for energy minimization studies. *J. Comput. Chem.*, 1999, **20**, 720–729; Halgren, T. A., MMFF VII. Characterization of MMFF94, MMFF94s and other widely available force fields for conformational energies and for intermolecular interaction energies and geometries. *J. Comput. Chem.*, 1999, **20**, 730–748.
21. Rizzo, R. C. and Jorgensen, W. L., *J. Am. Chem. Soc.*, 1999, **121**, 4827–4836; Jacobson, M. P., Kaminski, G. A., Friesner, R. A. and Rapp, C. S., Force field validation using protein side chain prediction. *J. Phys. Chem. B.*, 2002, **106**, 11673–11680.
22. Friesner, R. A. *et al.*, Glide: A new approach for rapid, accurate docking and scoring. 1. Method and assessment of docking accuracy. *J. Med. Chem.*, 2004, **47**, 1739–1749.
23. Halgren, T. A., Murphy, R. B., Friesner, R. A., Beard, H. S., Frye, L. L. Pollard, W. T. and Banks, J. L., Glide: A new approach for rapid, accurate docking and scoring. 2. Enrichment factors in database screening. *J. Med. Chem.*, 2004, **47**, 1750–1759.
24. Sherman, B., Day, T., Jacobson, M. P., Friesner, R. A. and Farid, R. A., Novel procedure for modeling ligand/receptor induced fit effects. *J. Med. Chem.*, 2006, **49**, 534–553.
25. Friesner, R. A. *et al.*, ExtraPrecision glide – Docking and scoring based on a new theory of molecular recognition. *J. Med. Chem.*, 2006, **49**, 6177–6199.

ACKNOWLEDGEMENTS. We thank Dr Shashidhar Rao, Schrödinger Inc. New York for training and help provided in using Schrödinger modelling tools. The anonymous referees are acknowledged for their critical comments on the manuscript.

Received 20 February 2007; revised accepted 21 August 2007